MODELLING OF THIN FILM MAGNETOIMPEDANCE SENSITIVE ELEMENT DESIGNED FOR BIODETECTION

Volchkov S.O.[1], Chlenova A.A.[1], Lepalovskij V.N.[1]

[1]Ural Federal University, Laboratory of Magnetic Sensors, Ekaterinburg, Russia

Abstract. Magnetic soft matter (ferrofluids or ferrogels) is one of the rapidly growing areas of research and applications including magnetic biosensing. Giant magnetoimpedance is the effect with proven capacity to magnetic label detection. In this work, we describe a universal model to simulate conditions of magnetic biodetection and to check its validity with giant magnetoimpedance sensitive element based on magnetic multilayer. Finite element method allows calculations of high-frequency current distribution using the Maxwell's equations taking into account the magnetodynamics of iron oxide water-based ferrofluid in small channels similar to the blood vessels. The modelling was realized with the licensed software Comsol©. The calculations were performed on a specialized engineering server based on four processors Intel Xeon E5 and 124 Gb RAM, adapted for parallel computations and suitable for description of individual layers with nanometer dimensions for the number of elements in the mesh structure above 10^6 cells. The designed model allows calculations of the current density, the outside magnetic flux, resistivity, etc. for each one of the created cells and total values by integration of sub-domains. One can quantitatively describe concentration of ferrofluid, velocity and pressure in the blood vessel. These changes affecting on the giant magnetoimpedance of the FeNi-based multilayer were both calculated and measured.

1 Introduction

Magnetic drug targeting (MDT) provide special opportunity to treat malignant tumours locally without systemic toxicity. An external magnetic field is focused on a particular region of interest to retain magnetic nanoparticles (MNPs) in form of water-based ferrofluids (FF) from the blood flow. MNPs can carry the chemotherapeutic agents to tumours for specific delivery. It is possible to use MNPs as a “carrier system” for a variety of anticancer agents (radionuclides, specific antibodies and genes) [1-2]. MDT is a complex process, where several phenomena concur: the pulsating blood flow that conveys the FF mix, its action on the vessels and muscular volume, and the interaction with an external magnetic field (due to the magnetization of the MNPs) aimed at prolonging the time of residence of the magnetizable drug carriers conveyed by the blood stream in the region of interest. Giant magnetoimpedance (GMI) is the effect which with proven capacity to quantify the presence of MNPs in the biological samples from model ferrofluids, ferrogels to in vitro grown cell cultures [3-4].

In this work we design a universal model to simulate conditions of magnetic biodetection in GMI FeNi/Cu/FeNi multilayers forming part of the “microstrip” transmission line with predetermined parameters, where impedance parameters are controlled by an external magnetic field. To confirm the model predictions, the real FeNi/Cu/FeNi GMI elements have been obtained and their impedance was measured in the installation mimicking the blood vessel conditions.

2 Modelling

The modelling and simulations were performed by finite element method (FEM) on licensed Comsol Multiphysics software version 5.0 The hardware implementation was realized with computer station having four CPU Intel Xeon E5, RAM 128 Gb and shared-memory parallelism architecture on Ubuntu 14.04 (Linux). The topology of the magnetic multilayered structure was developed in our previous experimental studies [5-7]. The GMI elements, the heterogeneous structures consisting of alternating layers of copper and permalloy onto the glass substrate: glass/ $[FeNi/Cu\_s]_4/FeNi/Cu\_c/[FeNi/Cu\_s]_4/FeNi$ (Fig. 1) were deposited by magnetron sputtering. The variation parameters were length, width and thickness of FeNi, Cu_c (copper central layer) and Cu_s (copper intermediate layers). The topological model of the multilayer was connected with the architecture model of the “microstrip” transmission line with SMA-adapters for calculations.

The topological model of “microstrip” line and FeNi-element was divided into sub-areas, which are tetrahedrons for 3D-configuration (Fig. 2(A)). The size of finite elements in the mesh partition depended on the wavelength of the electromagnetic excitation wave.

* Corresponding author: stanislav.volchkov@urfu.ru

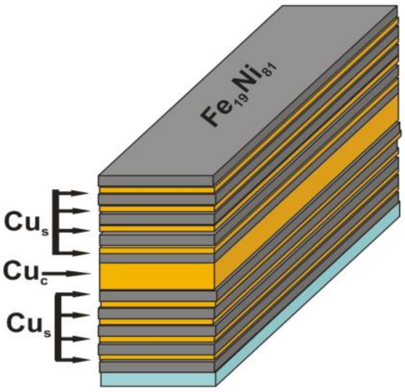

Figure 1. The topological model of the ferromagnetic multilayered film GMI element deposited onto glass substrate

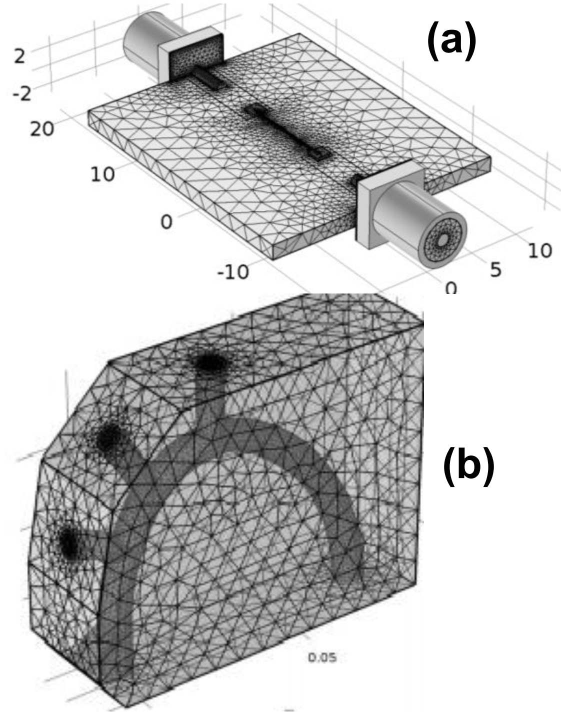

Figure 2. The mesh model of the GMI sensitive element placed in the microstip line with SMA adapters (a), blood vessel related part of the model (b).

A separate sub-grid of hexahedral elements was set for the boundary of the magnetic layer. This model used a transition boundary condition (TBC) programming function because of the need to incorporate the interface related to diffusion (1 nm) between the FeNi and Cu, layers and glass substrate as well as the propagation of electromagnetic waves for the layers with different dielectric and magnetic properties. For the numerical solution of FEM models we used frequency-dependent form of Maxwell's equations for waves with transmission electromagnetic mode (TEM) [7]:

$$\nabla \times \mu^{-1}(\nabla \times \vec{E}) - k_0(\varepsilon - \frac{j\sigma}{\omega\varepsilon_0})\vec{E} = 0 , \quad (1)$$

where E - electric field vector, μ - relative permeability tensor, ω is the angular frequency, σ is the conductivity tensor, ε is the relative permittivity tensor, and k_0 is the free space wave number. Microwave losses in the sample are introduced as permittivity and permeability anisotropic tensors. The model assumes that the static magnetic bias field (H_0) is much stronger than the alternating magnetic field of the microwaves. So the quoted expressions are a linearization for a small-signal analysis around this operating point. Following parameters of the materials have been used in the model: ε_{Sub} = 3.38 - dielectric permittivity of sample holder; ε_{SMA} = 2.10- dielectric permittivity of polytetrafluoroethylene in SMA-adapter; ε_{GS} = 4.80 - dielectric permittivity of glass substrate, σ_{hold}= 5.998 × 10^7 (S/m) -electrical conductivity of Cu in SMA-adapter and “microstrip” line roads; σ_{Cu}= 2.5 × 10^7 (S/m) electrical conductivity of Cus; σ_{FeNi}=6.6 × 10^6 (S/m) electrical conductivity of FeNi. Remaining volume in the model is air. An important step in the design of this microwave device is matching the characteristic impedance of total circuit (transmission line and sensitive element) to 50 Ohm through the parameters of variation. Impedance matching is equivalent to minimizing the reflections back to the input port [9].

Fig. 2(B) shows an example of the modelling of a portion of vascular system (the upper part of the aorta). Both aorta and its ramified blood vessels are embedded into a biological matrix (cardiac muscle). The following material properties were used: Blood - density = 1060 kg/m^3 - dynamic viscosity = 0.005 Ns/m^2; Artery - density is equal to 960 kg/m^3 - Neo-Hookean hyperelastic behavior: the coefficient μ is equal to 6.20 × 10^6 N/m^2, while the bulk modulus is equal to 20μ and corresponds to a value for Poisson’s ratio (ν = 0.45). An equivalent elastic modulus equals 1.0 × 10^7 N/m^2. Cardiac muscle - density = 1200 kg/m^3 - Neo-Hookean hyperelastic behavior: the coefficient μ equals 7.20 × 10^6 N/m^2, while the bulk modulus is equal to 20μ and corresponds to a value for Poisson’s ratio (ν = 0.45). An equivalent elastic modulus equals 1.16 × 10^6 N/m^2.

3 Experimental

The experimental multilayers glass/[FeNi(100 nm)/Cus(3 nm)]$_4$/FeNi(100 nm)/Cuc/[FeNi(100 nm)/ Cus(3 nm)]$_4$/FeNi(100 nm) were designed after simulations. They were deposited by magnetron sputtering in a magnetic field of 100 Oe onto 0.2 mm thick Corning glass 2875-25 substrates with dielectric permittivity ε=4.8. The composition of magnetic layer was $Fe_{19}Ni_{81}$. The formation of the GMI elements was carried out by metallic masks. Magneto-optical Kerr effect measurements confirmed formation of the well defined uniaxial magnetic anisotropy with easy magnetization axis oriented in plane of the elongated stripe sample along the short side, i.e. in the direction of the application of a magnetic field during the sample deposition. Small coercivity of about 0.5 Oe and anisotropy field of about 6 Oe – are typical features of soft ferromagnets. The impedance parameters were measured in 50 Ohm “microstrip” line by Agilent Impedance Analyzer follow standard procedure [9].

Table 1. Types of GMI experimental studies

Name	Type of GMI measurements
S1	Film
S2	Film with water capillary
S3	Film with FF capillary (concentration 0.02% = 1 g/l)
S4	Film with FF capillary (concentration 0.04% = 2 g/l)

For experimental studies of the FF dynamic behaviour the capillary was a tube of silicone with an outer diameter of 5 mm and an inner diameter of 3 mm of 1 m length. A motor working with of 4.5 V voltage pushed liquid through the capillary mechanically. The capillary was located perpendicular to the long side of the film parallel to the film plane (in the centre) at a minimum distance above the film. It was fixed without direct contact and therefore did not press the GMI element surface. Additional study confirmed that the operation of the motor does not affect the created external magnetic field features: both GMI curves for motor switch on and switch of curves were identical with an error of 1% for the GMI ratio of the total impedance. Series of the types of experimental studies are described in Table 1.

Commercial EMG 807 ferrofluid was de-aggregated for 10 min. for obtaining the desired concentrations in distilled water using ultrasonic bath. Initial concentration of the nanoscale iron oxide was 2 volume % [10].

4 Result and Discussion

The pressure values were defined as the mean values over a heart beating cycle with in substitution the blood sample by diluted FF. During a cycle the pressure varies between a minimum and a maximum values which are calculated using a relative amplitude. For the time-dependent analysis with FEM simulations, a simple trigonometric function is used for varying the pressure distribution and velocity over time (Fig 3).

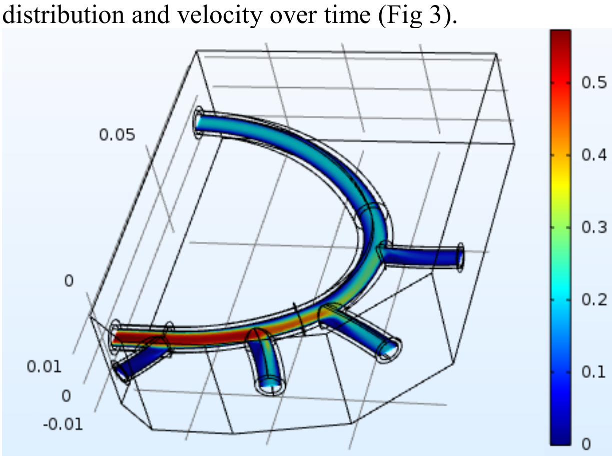

Figure 3. Velocity of Fe3O4 nanoparticles in a model of blood vessel (FEM modelling).

The transport and capture of MNPs in the channel under application of a magnetic field with different strength were calculated using the particle tracing module of finite element based COMSOL software. The dominant magnetic and fluidic drag forces are considered to predict the transport and capture of magnetic nanoparticles in a channel. Moreover, the diameter of tube and radius of MNPs are important parameters included in the model.

Fig. 5 shows FEM modelling results corresponding to different types of GMI experimental studies (S1-S4). One can see a good agreement for the frequency range below 180 MHz predicting the same GMI response for capillary with and without water. The highest difference between S1-S2 and S3, S4 responses was observed in a low frequency range below 110 MHz. Following

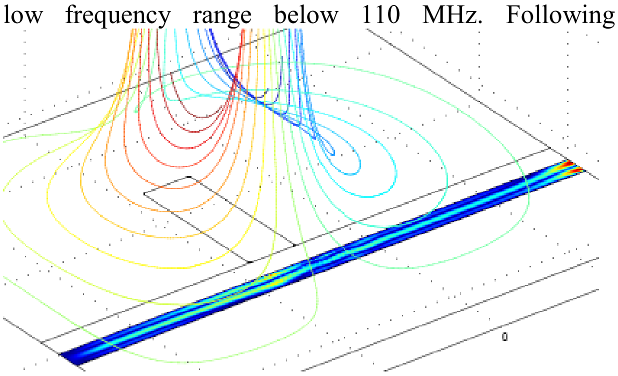

Figure 4. Magnetic flux distribution in a model system consisting of a blood vessel with FF and small magnet placed at a distance: thin film GMI element should be located in the gap between the magnet and the capillary.

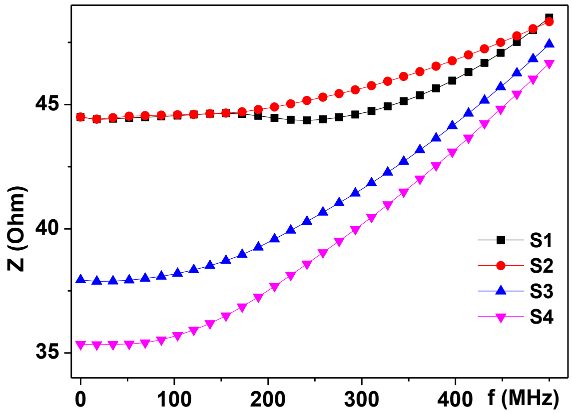

Figure 5. The modeling of frequency dependence of MI ratio of total impedance (a) and real part (b) for structure S1-S4

tendency was clearly observed: the higher the MNPs concentration, the lower the total impedance value for all frequencies under consideration.

Let us now analyze experimental results. Fig. 6 shows the frequency dependences of the maximum of the total impedance Z for all types of the measurements. In the case of Fig.6(a) Z(f) dependences are represented with the type of the measurements as a parameter and in the case of Fig.6(b) Z(Sx) are given for selected frequencies. Generally speaking, in a frequency range of 80 to 400 MHz we observe the same tendency as the tendency observed in the case of the modelling (Fig. 5): the higher the MNPs concentration, the lower the maximum value of the total impedance.

We must mention that the experimental values of the total impedance were approximately 2-3 times lower in comparison with the obtained by the modelling. One can clearly see that the deviation comes from the modelling of thin film GMI structure. As it was discussed before

[11] thick cooper conductor may cause formation a thick interface decreasing an effective conductivity and

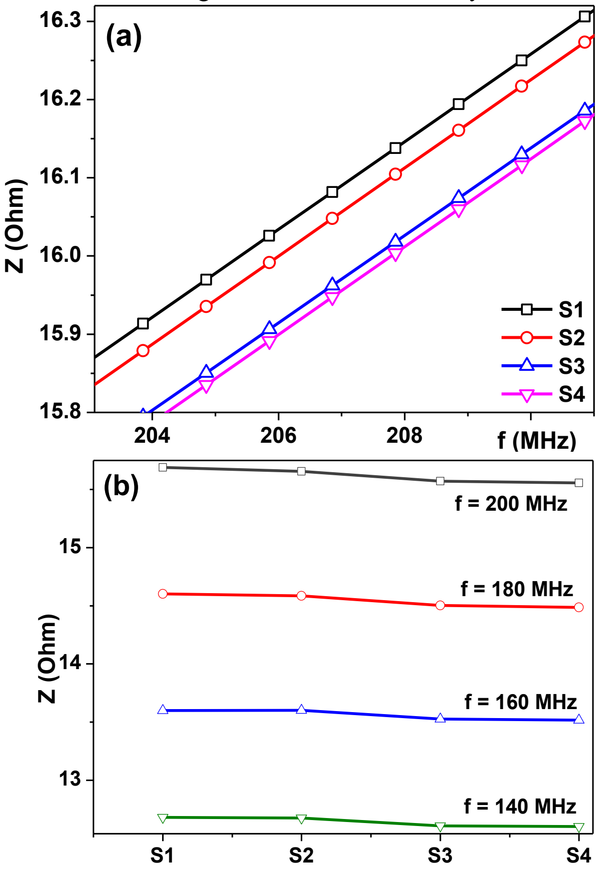

Figure 6. The experimental frequency dependence of the maximum of the total impedance Z of S1-S4 types of measurements. The summary of Z(Sx) given for selected frequencies (see also Table 1).

changing the current distribution. Although improvements of the GMI model are requested as the next step of the future research the general tendencies observed for the measurements of S1-S4 types shows reasonable agreement between the model and experimental results.

5 Conclusions

Universal model to simulate conditions of magnetic biodetection and to check its validity with GMI sensitive element based on magnetic multilayer was developed and tested. FEM allowed calculations of high-frequency current distribution using the Maxwell's equations taking into account the magnetodynamics of iron oxide water-based ferrofluid in small silicon channels mimicking the blood vessels. The calculations were performed on a specialized engineering server based suitable for description of individual layers of the GMI multilayered structure with nanometer dimensions for the number of elements in the mesh structure above 10^6 cells. Glass/[FeNi(100 nm)/Cu_s(3 nm)]$_4$/FeNi(100 nm)/Cu_c/[FeNi(100 nm)/Cu_s(3 nm)]$_4$/FeNi(100 nm) GMI multilayers were deposited by the magnetron sputtering. The designed model allowed calculations of the current density, the outside magnetic flux and resistivity for each one of the created cells and total values by integration of sub-domains. We were able to quantitatively describe behaviour of ferrofluids of different concentrations, flowing with certain velocity and under certain pressure in the blood vessel in the tube mimicking a capillary. These changes affecting the GMI of the FeNi-based multilayer were both calculated and measured showing the same tendency: the higher the MNPs concentration, the lower the total impedance value for all frequencies under consideration.

Acknowledgments

The research was supported by the Ministry of Education and Science of the Russian Federation Agreement no. 02.A03.21.0006. The some results were obtained within the framework of the state task of the Ministry of Education and Science of Russia 3.6121.2017/8.9. We thank Prof. F.A. Blyakhman for special support.

References

1. J. Llandro, J.J. Palfreyman, A. Ionescu, C.H.W. Barnes, Med. Biol. Eng. Comput. **48,** 977 (2010)
2. G.V. Kurlyandskaya, Iu.P. Novoselova, V.V. Schupletsova, R. Andrade, N.A. Dunec, L.S. Litvinova, A.P. Safronov, K.A. Yurova, N.A. Kulesh, A.N. Dzyuman, I.A. Khlusov, J. Magn. Magn. Mater. **431**, 249 (2017)
3. G.V. Kurlyandskaya, E. Fernandez, A.P. Safronov, A.V. Svalov, I.V. Beketov, A. Burgoa Beitia, A. Garcıa-Arribas, F.A. Blyakhman, Appl. Phys. Lett. **106,** 193702 (2015)
4. F. Blanc-Beguin, S. Nabily, J. Gieraltowski, A. Turzo, S. Querellou, P.Y. Salaun, J. Magn. Magn. Mater. **321**, 192 (2009)
5. G. V. Kurlyandskaya, A. García-Arribas, E. Fernández, and A. V. Svalov, IEEE Trans. Magn. **48(4)**, 1375 (2012).
6. A. Yuvchenko, V. N. Lepalovskii, V. O. Vas'kovskii, A. P. Safronov, S. O. Volchkov, G. V. Kurlyandskaya Technical Physics **59 (2)**, 230 (2014)
7. A. S. Antonov, S. N. Gadetskii, A. B. Granovskii, A.L. D´achkov, V.P. Paramonov, N.S. Perov, A.F. Prokoshin, N.A. Usov, A.N. Lagar´kov, Fiz. Met. Metalloved. **83 (6)**, 60 (1997).
8. L. D. Landau and E. M. Lifshitz, Course of Theoretical Physics, Vol. 8: Electrodynamics of Continuous Media (Nauka, Moscow, 1982; Pergamon, New York, 1984).
9. G.V. Kurlyandskaya, D. de Cos, S.O. Volchkov, Russ. J. Nondestruct. Test. **4,** 377 (2009)
10. https://ferrofluid.ferrotec.com
11. G.V. Kurlyandskaya, A.A. Chlenova, E. Fernández, K.J. Lodewijk J. Magn. Magn. Mater. **383**, 220 (2015)